SCREENING OF POTENTIAL ANTI-INFLUENZA AGENTS FROM *JUGLANS MANDSHURICA* MAXIM. BY DOCKING AND MD SIMULATIONS

Y. YANG[a,*], Z. YANG[b, *], J.LIU[c], F.WU[b],X.YUAN [d]
[a]*Forestry Academy of Jilin province, Changchun 130033, China*
[b]*School of Basic Medical Sciences, Jiamusi University, Jiamusi 154007, China*
[c]*College of Food Science and Engineering, Jilin Agricultural University, Changchun 130118, China*
[d]*Institute of Biomedicine, Jinan University, Guangzhou 510632, China*

Docking and molecular dynamics simulations were performed on the interactions between 35 chemical constituents of *Juglans mandshurica* Maxim. and the surface glycoproteins of influenza virus (hemagglutinin and neuraminidase), in order to understand the bindings and design dual-targeting drugs. It was found that hyperin, avicularin, juglanin, isoquercetin and α-tetralone-5-G-glucopyranoside have obvious binding specificities to hemagglutinin (H7) and neuraminidase (N9). The interaction energies (E_{int}) of the top 5 hits with H7 (N9) were -45.04 (-59.97), -41.23 (-64.06), -43.25 (-60.10), -47.70 (-66.29) and -43.11 (-49.34) kcal mol^{-1}, respectively. The residues GlyA124, AlaA125, ThrA126 and TrpA142 of H7, and residues Asp151, Arg152, Arg156 and Trp178 of N9 played the most significant role for the bindings. Furthermore, the binding footprints revealed the key structural variables which should be more guarded in the rational drug designs. Compared with other candidates, isoquercetin is a potential source of anti-influenza ingredient, with better interaction energy and advantages over conventional agents. This work also pointed out how to effectively reinforce the susceptibility of inhibitors to influenza virus.

(Received November 15, 2014; Accepted January 9, 2015)

*Keywords:*Influenza surface glycoproteins;Antiviral agents;*Juglans mandshurica* Maxim.;Docking; Molecular dynamics

1. Introduction

Influenza A virus reservoirs in birds and certain mammals have deprived millions of lives, and constantly introduced possible public health threat[1-2]. It has been established that many infection cases appear to have a link to severe respiratory illness[3]. As of August 31, human cases of H7N9 in China reached 134, with the mortality rate of 34%[4]. So far, commercial neuraminidase (NA) inhibitors remain the primary drugs prescribed to the infected persons [5]. While, the frequent emergences of drug-resistant cases[6-7] and limited drug administrations[8]have spurred the search to explore novel anti-influenza agents.

There are two principal surface glycoproteins of influenza virus, hemagglutinin (HA) and neuraminidase (NA), which reflect the antigenic diversity of viruses [9]. According to the two proteins, the influenza A viruses can be further divided into over one hundred serological subtypes; for example, H7N9 identifies it as having HA of the H7 subtype and NA of the N9 subtype. Up to present, 17 serotypes of HA (H1-H17) and 10 serotypes of NA (N1-N10) have been identified[10]. HA mediates the binding of viral particles to the sialic acid receptors on the cell surface and the entry of virus into the host cell [11-12]; NA is responsible for the cleavage of sialic acid residues, thereby is of great relevance for the release of progeny virus and enhancing their infection efficiencies[13-14]. The two glycoproteins are attractive targets for the rational drug designs [15],

* Corresponding author:yang-yu-chun@163.com (Y. C. Yang), yzws-123@163.com (Z. W. Yang)

and much efforts have been devoted to develop inhibitors that target both of them, which be deemed to reduce resistance issues resulting from the mutations [15-16].

Traditional Chinese medicine(TCM) compounds play a fundamental role in clinical practice, and show a potential in the therapy of influenza [17-18].Many studies on screening anti-influenza active constituents have been carried out with the chemical and pharmacological experiments[17-22], and some novel agents have been validated, including a variety of polyphenols and flavonoids[17-24].Most of them show potentials to serve as the HA and NA inhibitors individually; e.g. the polyphenols of *Camellia sinensis*[21] and trihydroxymethoxyflavone analogues [25].Recently, three novel compounds derived from *Rosemarinus officinalis* and *Guatteria amplifolia* have been identified with the dual binding properties to the HA and NA proteins, with the aid of computational approaches [16]. Besides, previous studies revealed that 2-cyclohexene-1, 4-dione ring of natural phenolic compound juglone, has the binding specificity to both of HA and NA proteins[22]. These developments give rise to the attractive candidates of dual-targeting drugs for influenza.

Receptor-based virtual screening, including docking and molecular dynamic (MD) simulations, has been shown to effectively improve enrichment factors in the identification of lead compounds[16, 26].Meanwhile, characterizing binding for inhibitors with target proteins will contribute to the in-depth understanding, and ultimately enable the design of improved agents[5, 27].Our previous studies have indicated that natural extracts of *Juglans* can be employed to design as the dual-targeting inhibitors for influenza [22].In this study, aforementioned computational tools were utilized to evaluate the interactions between chemical constituents of *Juglans mandshurica* Maxim.(Scheme 1) and the HA and NA proteins of 2013 A/H7N9 influenza virus. The top five candidates were selected by the prediction models, and further energetic and geometric analyses are carried out in order to study the detailed interaction profiles and reveal the import functional groups. We hope that the results can be useful for the drug development.

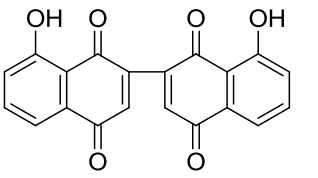

1

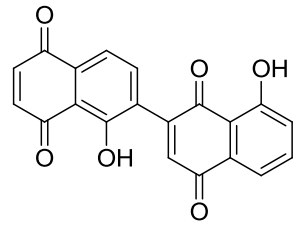

2

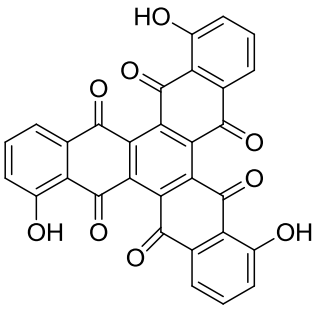

3

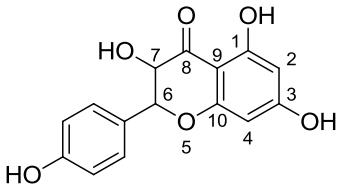

4

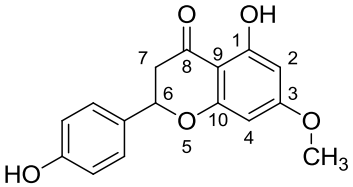

5

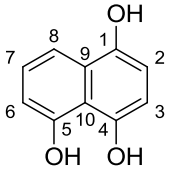

6

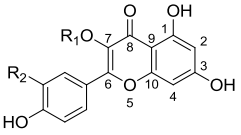

	R1	R2
7 (hyperin)	-*β*-D-galp (SRSRR)	-OH
8 (avicularin)	-*α*-L-ara	-OH
9 (juglanin)	-*α*-L-ara	-H
10	-H	-H
11	-H	-OH
12 (isoquercetin)	-*β*-D-galp (SRSSR)	-OH

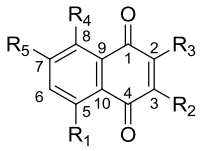

	R1	R2	R3	R4	R5
13	-H	-H	-H	-H	-H
14	-OH	-H	-H	-H	-H
15	-H	-H	-Me	-H	-H
16	-OH	-H	-Me	-H	-H
17	-OH	-Me	-H	-H	-H
18	-OH	-Me	-Me	-H	-H
19	-OH	-H	-H	-OH	-H
20	-OH	-CH_3O	-H	-H	-Me
21	-OH	-H	-CH_3O	-H	-H

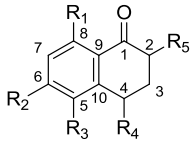

	R1	R2	R3	R4	R5
22	-H	-H	-OH	=O	-H
23	-H	-H	-OH	=O	-Me
24	-OH	-H	-H	-OH	-H
25	-H	-H	-G	-OH	-H
26	-*β*-D-glc	-H	-H	-OH	-H
27	-OH	-H	-OCH_3	-OH	-H
28	-H	-H	-H	-OH	-H
29	-H	-H	-OH	-OCH_3	-H
30	-OH	-H	-OH	-OCH_3	-H
31	-H	-H	-*β*-D-glc	-OH	-H
32	-H	-H	-OH	-OH	-H
33	-H	-H	-H	-*β*-D-glc	-H
34	-OH	-H	-OH	-*β*-D-glc	-H
35	-H	-OH	-H	-H	-H

Scheme 1.Chemical constituents of Juglans mandshurica Maxim. used in this study

2. Materials and Methods

2.1. Validation of protein structures

The HA protein structure of 2013 A/H7N9 virus(PDB entry: 4BSE, 2.55Å resolution) [28]was retrieved from the RCSB Protein Data Bank (http://www.rcsb.org). As to the NA protein, the amino acid sequence has been released in the NCBI database (Accession No. AGI60300.1)[29], but its crystal structure is not yet solved. Thus, the NA protein structure of recent A/H7N9 virus was built throughout the homology modeling protocol within Discovery Studio software package[30-31]. An entry of 1F8B in PDB (N9 subtype, 1.8 Å resolution)[32] was selected as the template, with similarity 81.9% to the NA protein of recent A/H7N9 virus. The calcium ion (Ca^{2+}) near the active site was reserved [33-35].For convenience, the protein structures are named as H7 and N9 throughout this work.

All the proteins were saturated with hydrogen atoms, based on the expected charge distributions of amino acids at physiological pH[33-35].The energy minimizations were performed by a 500-step steepest descent minimization, followed by conjugate gradient minimization, until converged to 0.01 kcal·mol^{-1}·Å^{-1}.Note that the energy-minimized N9 protein was further refined by 5.0 ns explicit solvent MD simulations in the NPT ensemble (300 K, 1 atm), using GROMACS4.5.3 program[36]and Charmm27 force field [37], as recommended elsewhere[22, 31, 38]. Details of the MD simulation setup are in agreement with reference[38] or refer to section 2.2.

2.2.Docking and MD simulations

In accord to the previous reports [39-40], virtual screening process was performed using the cDocker module[41] in Discovery Studio, features for its grid-based method that the residues are held rigid and ligands are free to move. The "Minimize Ligands" tools [30]were used to handle the geometry and partial atomic charges of chemical constituents (collected from reference[42], Scheme 1), using the Charmm force field [37, 43], with a convergence criterion of 0.001 kcal·mol^{-1}·Å^{-1}.The binding site sphere was assigned with a sphere of 10.0 Å. Combining random rotations and simulated annealing method, the optimal orientations of ligands within H7 and N9 were probed, on the basis of interaction energies and geometrical matching qualities[39-40]. The optimal docked complexes were then minimized, until converged to 0.01 kcal mol^{-1} Å^{-1}.

The energy-minimized docked complexes were sufficiently equilibrated by 10.0 ns MD simulations, using GROMACS4.5.3 program [36] and GROMOS96 43a1 force field [36, 44]. Each docked complex was placed in a SPC/E (simple-point-charge) water box, with a distance of 9.0 Å extended from any solute atom. Cl^-counter-anions were placed to neutralize the system [45]. The NPT ensemble was applied (300 K, 1 Bar)[46], and the particle-mesh Ewald (PME) method was applied to handle the long-range electrostatics [47]. The coulomb and vdW cutoff radii were set to 8.0 and 14.0 Å, respectively. The LINCS algorithm was applied to constrain all bonds involving hydrogen atoms [48]. The MD trajectories were saved every 10.0 ps, with time step of 2.0 fs. The average structures of the 8.0~10.0 ns MD trajectories were used for analysis.

3. Results and discussion

3.1. Structural variability and virtual screening hits

N9 structure was generated with the template (PDB ID: 1F8B) via the MODELER module[30, 49], and further refined by the solvated 5.0 ns MD simulations. In accord with our previous work [31], the model structure is structurally close to the template. As a result of its good structural compatibility and stereochemical features [31], it should be reasonable and could be used to study the interactions with various chemical constituents. A series of 35 chemical constituents were independently docked into the H7 and N9 proteins and screening results after each filtering step were summarized in Table 1.Only hits that have the interaction energy below -40.0 kcal mol^{-1}were selected from each set, and the ultimately selected 5 compounds were indicated in bold, see Table 1.

Table 1. The cDocker energy (E_{total}) and cDocker interaction energy (E_{int}) between proteins and various chemical constituents[a]

Constituent[b]	H7		N9	
	E_{total}	E_{int}	E_{total}	E_{int}
1	-18.86	-29.61	-29.56	-49.20
2	-21.66	-29.99	-32.43	-48.88
3	-7.51	-35.65	-12.74	-47.30
4	-23.74	-34.91	-31.63	-43.24
5	-21.47	-32.84	-26.24	-41.81
6	-6.51	-19.84	-17.57	-30.91
7	**-8.39**	**-45.04**	**-18.70**	**-59.97**
8	**-5.26**	**-41.23**	**-25.22**	**-64.06**
9	**-1.69**	**-43.25**	**-10.86**	**-60.10**
10	-23.40	-28.02	-32.16	-40.51
11	-26.44	-30.19	-37.03	-43.85
12	**-9.61**	**-47.70**	**-26.76**	**-66.29**
13	-13.12	-15.69	-23.26	-25.96
14	-15.33	-17.62	-23.85	-30.01
15	-9.06	-19.03	-15.81	-26.05
16	-8.89	-19.95	-19.33	-30.40
17	-11.47	-20.90	-17.87	-31.33
18	-1.94	-22.49	-10.38	-30.73
19	-17.36	-19.22	-26.62	-32.95
20	-18.05	-22.42	-26.79	-37.51
21	-15.53	-21.41	-23.34	-33.67
22	-14.60	-19.36	-24.65	-33.17
23	-15.15	-20.52	-22.87	-33.30
24	-16.88	-21.07	-25.46	-33.67
25	**-6.72**	**-43.11**	**-14.15**	**-49.34**
26	-10.94	-34.01	-16.36	-45.65
27	-13.42	-21.24	-25.23	-35.86
28	-17.24	-20.85	-22.21	-26.18
29	-17.04	-21.42	-27.35	-34.78
30	-18.87	-22.11	-30.16	-36.08
31	-12.92	-31.32	-21.76	-46.78
32	-18.26	-22.16	-28.34	-32.90
33	-13.50	-28.53	-26.02	-50.06
34	-14.10	-33.17	-29.82	-53.06
35	-17.21	-21.00	-25.53	-30.49

[a] Energy units in kcal mol^{-1};

[b] Chemical structures can be found in Scheme 1.

The selected 5 hits could be docked to the receptor binding domain (RBD) of H7, which is mapped to the globular head of receptor[22, 28]; at the same time, they are able to enter and fill the cavity of N9 drug binding pocket (Fig. 1). Among the 5 compounds, com7 (hyperin), com8 (avicularin), com9 (juglanin) and com12 (isoquercetin) are flavonoids, while com25 (α-tetralone-5-G-glucopyranoside) is a polyphenol compound, with the core template of 4-hydroxy-3,4-dihydronaphthalen-1(2H)-one (Scheme 1).With the conformation diversity, the binding properties of the 5 hits somewhat differ from each other, which will be discussed in the following section.

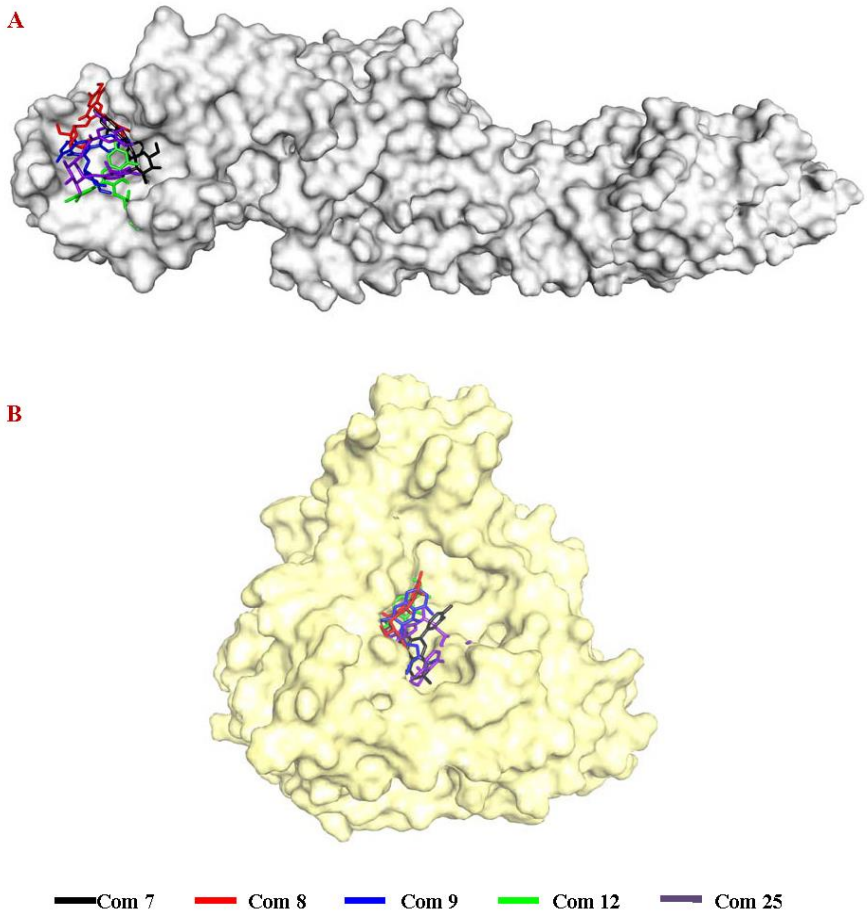

Fig. 1. Selected hits clustered in A) H7 and B) N9
The Connolly surfaces of H7 (in grey) and N9 (in chalky yellow) are created using the Discovery Studio scripts. The selected hits are represented by stick models

3.2. Characteristics of compound binding poses

To provide comprehensive analysis of the interactions involving the top5 hits with target proteins, MD simulations were performed to refine each model[50-52].Their potential energies remain rather stable throughout the simulation time (Fig. 2). Root-mean-square deviation (RMSD) is a widely used way to determine the equilibrium state of a system [53]. In our simulations, no obvious fluctuations are observed for the backbone-atom RMSD of docked complexes since about 8.0 ns (Fig. 3), consistent with previous MD results [21-22, 54]. Accordingly, the geometric and energetic analyses are made on the average structures of 8.0~10.0 ns MD trajectories.

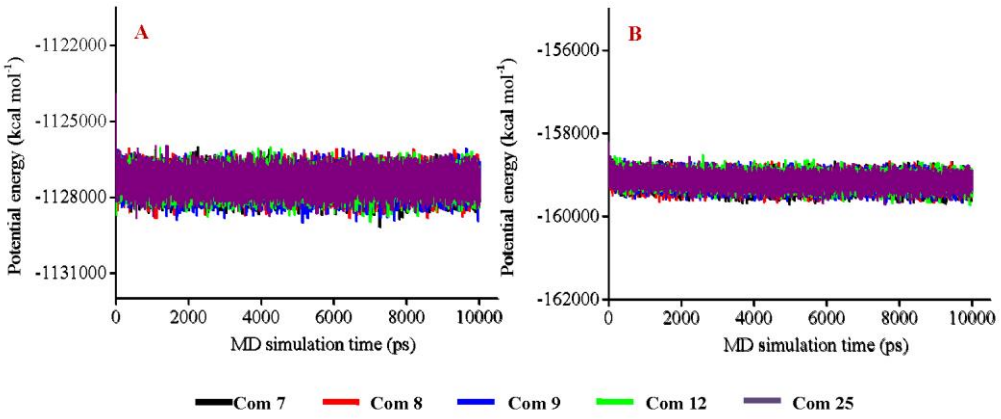

Fig. 2. Potential energy plots of the docked complexes with respect to simulation time: A) compound-H7 and B) compound-N9

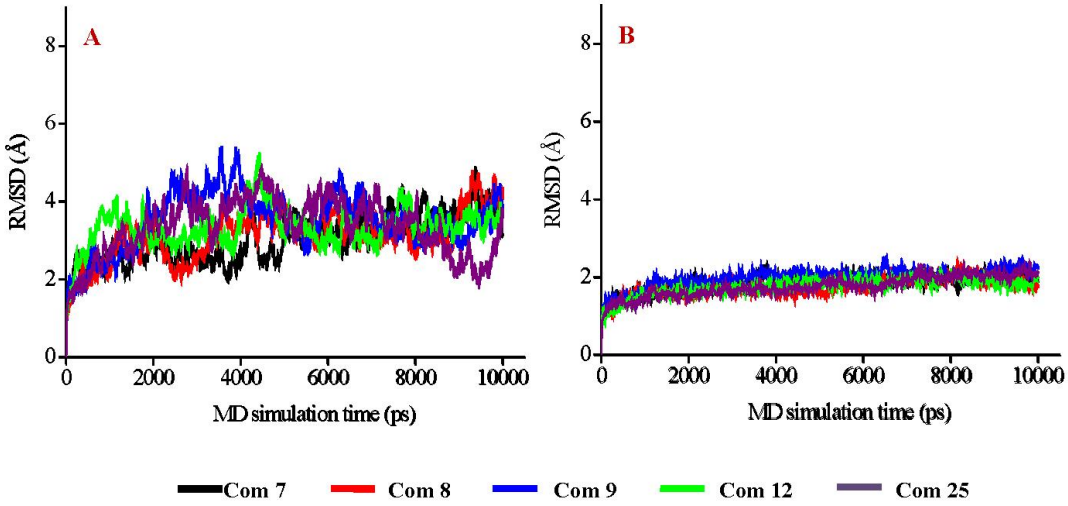

Fig. 3. Backbone-atom RMSD of the docked complexes in 10ns MD simulation: A) compound-H7 and B) compound-N9

As revealed by Fig.4, the 5 hits pose the similar location in the binding pocket of H7, whereas their space orientations somewhat differ from each other. The binding pose of com7 within H7 was characterized by the presence of two H-bonding interactions involving the hydroxyl groups with residues ThrA126 and GlyA216 (Fig. 4A). Additionally, two H-bonds were formed between oxygen atoms of methoxymethane groups (-C-O-C-) and residues TyrA88 and ThrA126 (Fig. 4A). As for com8, its core template 5,7-di(l1-oxidanyl)-4H-chromen-4-onewas bound towards residue TrpA142, with the strong π-π stacking; and its tetrahydro-2H-pyranring was stabilized by residuesGlyA124, AlaA125 and ThrA126, with the relatively strong non-polar interactions (Fig. 4B). As compared to com 7 and com 8, com 9 somewhat deviates from the H7binding site, with less directly contacting residues (Fig. 4C).The structure of com12 is very similar as that of com 7, merely with the chirality diversity of hydroxyl group at the counterpoint site of β-D-galp (S vs. R). Thetetrahydro-2H-pyranring of com 12 is slimly unfavorable to the H7 binding, so H-bonding interactions with residues ThrA126 and GlyA216 were lost(Fig. 4D). However, com 12 was surrounded and well fitted by residues GlyA124, AlaA125, ThrA126, TrpA142, LysA184 and LeuA185, throughout the hydrophobic interactions (Fig. 4D). Regarding

as com 25,its core template4-hydroxy-3, 4-dihydronaphthalen-1(2H)-one was docked towards residues GlyA216 and SerA218, the side chains of com 25 may form the hydrophobic interactions with the adjacent residues GlyA124, AlaA125, ThrA126, TrpA142, LysA184 and LeuA185 (Fig. 4E). The interaction energies (E_{int}) of the 5 hits with H7 are evaluated at -45.04, -41.23, -43.25, -47.70 and -43.11kcalmol^{-1}, respectively (Table 1).

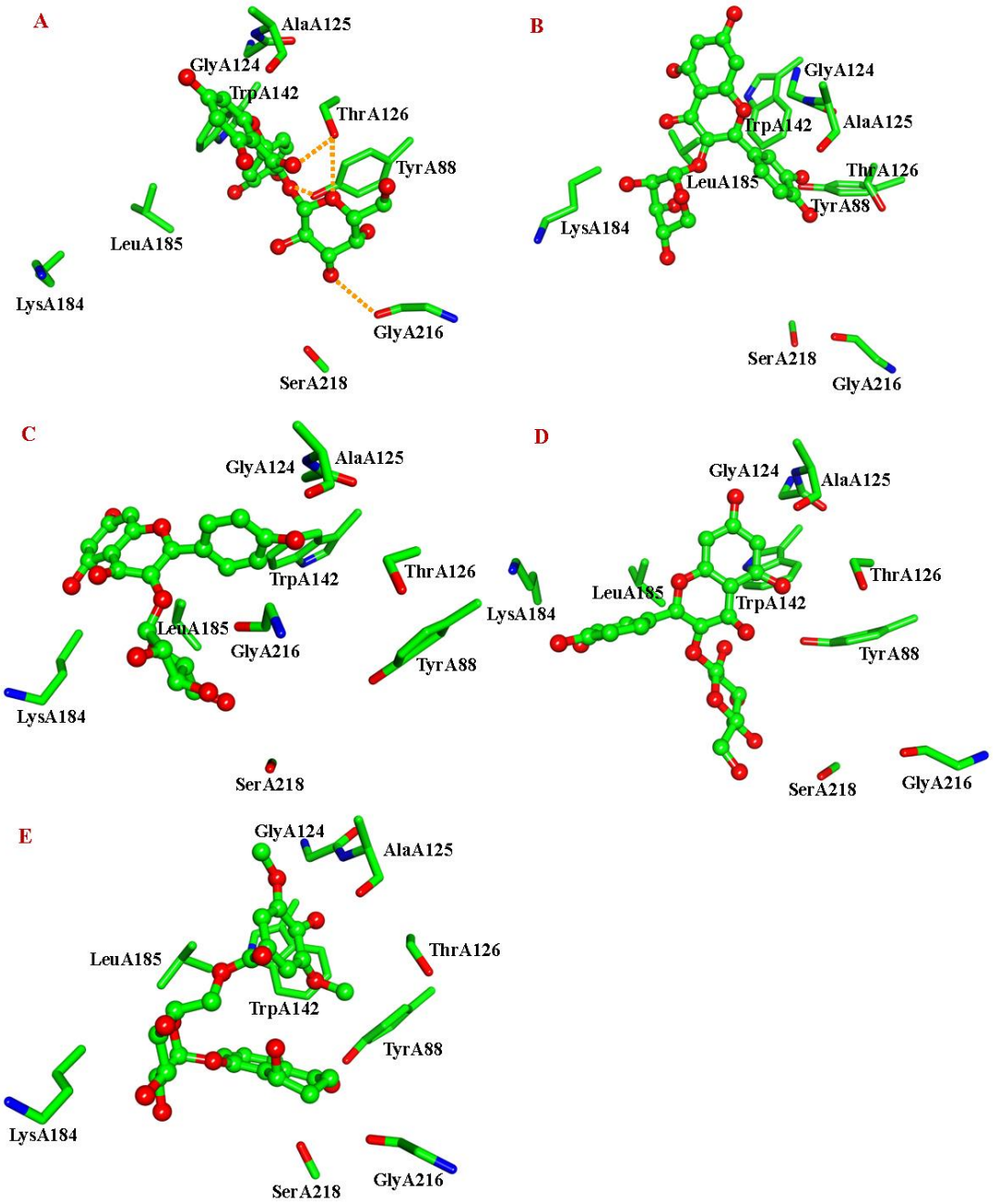

Fig. 4. Views of the binding modes of the H7 binding-pocket residues with the compounds: A) Com 7, B) Com 8, C) Com 9, D) Com 12 and E) Com 25 Key residues and compounds are represented by stick, and ball and stick models, respectively. The C, N and O atoms are colored in green, blue and red, respectively. The important H-bonds are labeled in the gold dashed lines

To expediently elaborate the binding distinctions, the interactions of N9 with oseltamivir carboxylate (OC) were described firstly (Fig. 5)[5, 15]: Carboxylate anion of OC was docked towards arginine triad Arg118, Arg292 and Arg371, with the electrostatic and H-bonding interactions; Amino and N-acetylamino groups of OC were observed to engage the H-bonds

networks with residuesGlu119, Asp151 and Arg152; OC ethylpropoxy group was stabilized by residues Glu276 and Glu277. As shown in Fig. 5, the 5 hits pose the position similar to that of OC, with the different binding properties. Regarding as com 7, the benzene ring of com 7 was docked towards residue Arg371, with one H-bond; its 5,7-di(l1-oxidanyl)-4H-chromen-4-one and tetrahydro-2H-pyran rings were further stabilized by residues Arg152, Ala246, Glu276 and residues Arg156, Trp178, via numerous H-bonds(Fig. 6A).The binding pose of com 8 within N9 is rather far to that of OC (Fig. 6B)[55], and its benzene ring was oriented towards residues Arg156 and Trp178 along with the formation of two and one H-bonds, respectively. The 5,7-di(l1-oxidanyl)-4H-chromen-4-one of com 9 was stabilized through H-bonding interaction with residue Arg118 (Fig. 6C).Com 12 in the binding pocket of N9 is characterized by the strong electrostatic interactions involving the hydroxyl groups (benzene and tetrahydro-2H-pyran rings), methoxymethane group (-C-O-C-) and carbonyl group (C=O) with the residues Asp151, Gln226, Arg156 and Tyr406 (Fig. 6D), with the formation of each one H-bond, and similar as the case of OC[34, 56].Compared with the 5,7-di(l1-oxidanyl)-4H-chromen-4-one core of com 7, 8, 9 and 12, com 25 has a central 4-hydroxy-3, 4-dihydronaphthalen-1(2H)-one ring (Scheme 1). Despite differences in chemical compositions, com 25 has the similar binding model with N9 (Fig. 6E): the electrostatic interactions were observed between hydroxyl groups of com 25 and residues Arg292, Asn294, Gly348, Arg152, associated as four H-bonds. The interaction energies (E_{int}) of the 5 hits with N9 are equal to -59.97, -64.06, -60.10, -66.29 and -49.34 kcalmol^{-1}, respectively (Table 1).

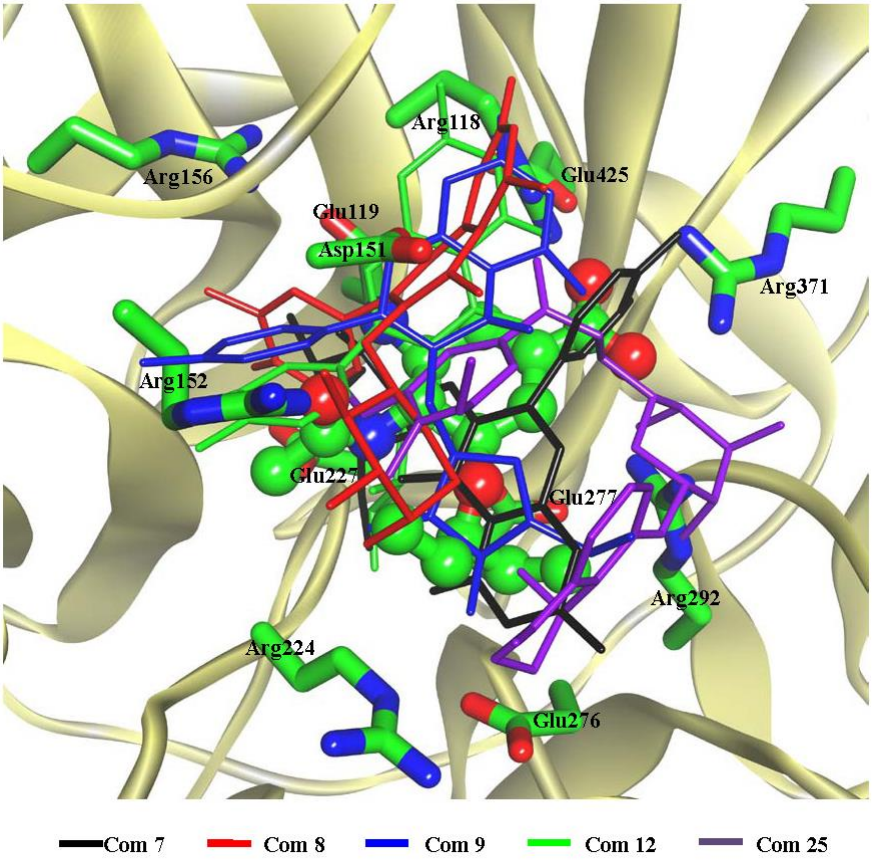

Fig. 5. Top five hits superposed at the N9 binding pocket following 10 ns MD simulations Key residues and compounds are represented by stick models. The binding pose of oseltamivir carboxylate (OC) with N9 is also shown with the ball and stick model. The C, N, O atoms of residues and OC are colored in green, blue and red, respectively

3.3.Implication for dual-targeting drug design

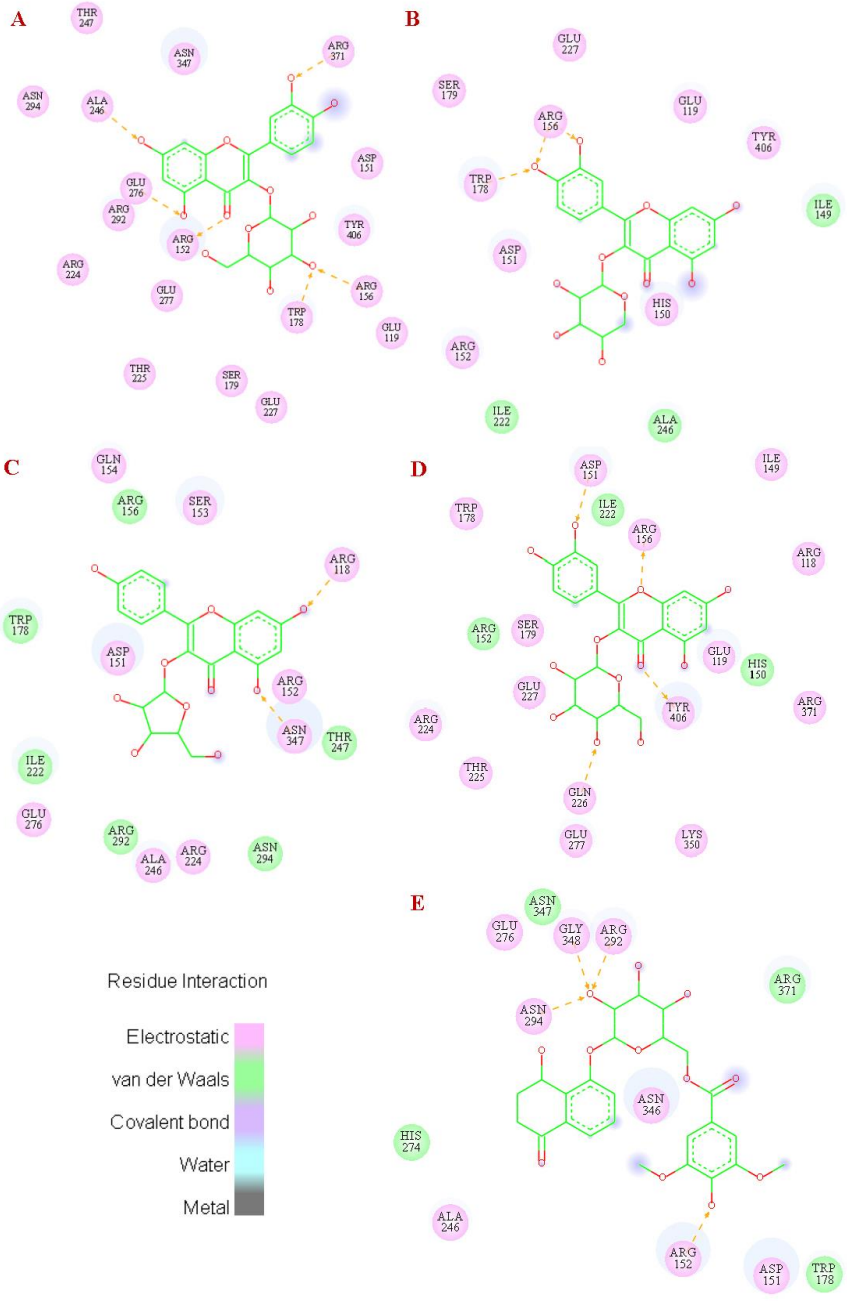

Fig. 6.Interactions between N9 and compounds are illustrated for A) Com 7, B) Com 8, C) Com 9, D) Com 12 and E) Com 25 Hydrogen bonds are indicated by gold dashed lines between the atoms involved

As described above, the interesting structural finding entails 5 chemical constituents from *Juglans mandshurica* interacting within the binding pockets of H7 and N9. It indicated that the numbers of H-bonds and binding poses of the 5 hits differ from each other, a result of the structural differences (Figs. 4 and 6). Nonetheless, there are some common characteristics of the bindings. The residues GlyA124, AlaA125, ThrA126 and TrpA142 of H7 all represented strong interactions in the bindings (Fig. 4). It means that the four residues may be the key for the inhibitions and should be given enough attention in the drug designs[21-22, 57-58]. In addition, all of 5 hits were observed to engage the electrostatic interactions with the positively charged pockets consisting of residues Arg118, Arg292 and Arg371(N9 protein), consistent with reported NA inhibitor bindings

[21-22, 31, 33-35]. The catalytic residuesAsp151 and Arg152 are critical for the functions of NA proteins, and residue Arg156 and Trp178 are crucial to the stabilizations of the NA active sites [5, 15, 59]. As the interactions in Fig. 6 indicated, the four residues play an important role for the bindings. In addition, the mutations of the four residues have received the most attention and exert observable influences on the drug designs [5, 59-61].

The top 4 derivatives (com 7, 8, 9 and 12) have in common a core template of 5,7-di(l1-oxidanyl)-4H-chromen-4-one and numerous hydroxyl groups addition to their native structures (Scheme 1). Among them, com 12 has the largest interaction energies with both of H7 and N9 (-47.70 and -66.29 kcal mol^{-1}), and its binding with N9 is more close to those of current NA drugs (Figs. 5 and 6D) [5, 59, 62].The hydroxyl group addition seems to play an important role in the bindings and be the main explanation for stronger inhibition activity of com 12, consistent with the experimental reports showing that decreasing the number of hydroxyl groups of compounds results in a reduction of inhibitory activities [63-64]. Com 7 and 12 merely differ by the chirality diversity of hydroxyl group(R vs. S, Scheme 1), but the differences in binding poses(Figs. 4 and 6) and E_{int} values (Table 1) suggest that the chirality of hydroxyl group has the influence on the bindings. This issue has be aroused by the thalidomide tragedy that (S)-thalidomide is a teratogen, and quite contrary to its (R)-stereoisomer, an effective sedative [65]. Hence, the chirality of candidates should be given enough attention in the drug designs [35].Besides, the long side chain (-G) of com 25 has less complementary properties against the geometrical and biophysical environment of the H7 and N9 binding pockets (Figs. 4 and 6), and should be more guarded in the designs of anti-influenza agents.

Contour of the top 5 hits at 10 ns MD simulation to the relative spatial positions of structural feature maps are shown in Fig. 7, with oseltamivir carboxylate (OC) also displayed in aid of visualization. It was found that the descriptor variables hydrophobic group, hydrogen-bond donor and hydrogen-bond accepter, are appropriate to describe the interaction mode of 5 hits within H7 and N9, as well as the field properties around the hits(Fig. 7). In terms of electrostatistics in this model, one highly polar region is worth noting. This area corresponds to the acidic pocket where the carboxylate anion of OC has strong ionic (H-bonding) interactions with a triad of arginine residues in N9: Arg118, Arg292 and Arg371[5, 59, 62]. In addition, the model tends to have two prominent hydrogen-bond donors, which can meet the electrostatic requirement of a charged environment, such as residues Glu119, Asp151 and Arg152 of N9. One hydrophobic group accords well with the properties of a hydrophobic pocket formed by the surrounding residues Glu276 and Glu277 for N9, or the residues GlyA124, AlaA125 and ThrA126 for H7 (Figs. 4, 6 and 7). These descriptor variables have been usually kept constant in the NA inhibitor structural optimization[5, 59, 61, 66].

Key binding locations of the 5 hits include residues GlyA124, AlaA125, ThrA126 and TrpA142 for H7, and residues Asp151, Arg152, Arg156 and Trp178 for N9 (Figs. 4 and 6). Mutations currently attributed to drug resistance are focused on the residues His274 and Asn294 of the NA proteins [67], and the residues Glu190, Gln226 and Gly228 of the HA proteins [68]. Since the key binding locations do not overlap with the residues prone to mutation, the 5 hits would likely be able to exert activity across these variants, especially com 12. Thus, com 12 may be an attractive lead compound for designing novel dual-target inhibitors. Furthermore, based on the results and observations of this study, the additional hydroxyl group or analogy hydrogen donors may fit the dual binding pockets, such as amino or guanidino group; the negatively charged groups (e.g. carboxylate group) may confer up to the improved binding profiles [5, 15], and probably confer a higher bioactivity.

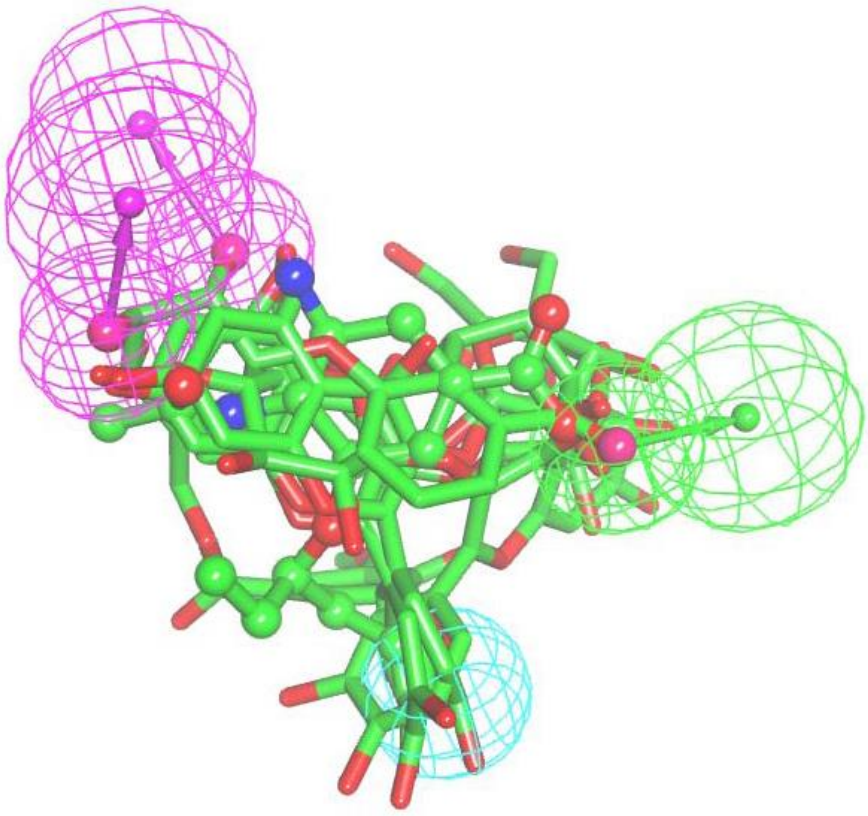

Fig. 7. Pharmacophore features of the top five hits Hydrophobic group, hydrogen-bond donor and hydrogen-bond accepter are colored in light-blue, magenta and green, respectively. Hits are shown with the stick models, oseltamivir carboxylate (OC) is highlighted in ball and stick model

4. Conclusions

Multiple anchors suggest that polyphenols and flavonoids may be the resistant to drug resistance and raise a new idea to treat influenza. In this work, docking and MD methods were combined to study the bindings involving 35 chemical constituents of *Juglans mandshurica* Maxim.(Scheme 1) with the HA and NA proteins of 2013 A/H7N9 influenza virus.

Among the 35 compounds, com 7 (hyperin), com 8 (avicularin), com 9 (juglanin), com 12 (isoquercetin) and com 25 (α-tetralone-5-G-glucopyranoside) have rather obvious binding abilities to the H7 and N9 proteins. The interaction energies(E_{int}) of selected 5 hits with H7(N9) are evaluated at -45.04 (-59.97), -41.23 (-64.06), -43.25 (-60.10), -47.70 (-66.29) and -43.11 (-49.34)kcalmol^{-1}, respectively(Table 1). Details of the binding specificity are given in the section 3.2. According to the energetic and geometric analyses, key binding locations of the 5 hits include residues GlyA124, AlaA125, ThrA126 and TrpA142 for H7, and residues Asp151, Arg152, Arg156 and Trp178 for N9 (Figs. 4 and 6). Furthermore, the binding footprints reveal that the hydroxyl group addition, the chirality diversity of hydroxyl group and long side chain (-G) should be more guarded in the designs of anti-influenza agents. Besides, the descriptor variables hydrophobic group, hydrogen-bond donor and hydrogen-bond accepter, are appropriate to describe the properties around the hits. Among the 35 constituents, com 12 shows its potential, with better interaction energy(E_{int}) and advantages over conventional agents such as oseltamivir. In addition, the modifications were explored compared with the properties of the surrounding residues of HA and NA proteins. We hope that the results will be helpful for designing novel dual-target inhibitors for influenza virus.

Acknowledgement

We are grateful for the financial supports from Forestry industry research special funds for public welfare projects (No. 201104040), National Natural Science Foundation (No. 31200429), Jilin Province Science and Technology Development Plan Project (No. 20100934 and 20100260) and Scientific Research Foundation of Heilongjiang Provincial Education Department (No. 12531690).

References

[1] E.Bautista, T.Chotpitayasunondh; Z.Gao; S. A.Harper; M.Shaw; T. M.Uyeki; S. R.Zaki; F. G.Hayden; D. S.Hui; J. D.Kettner; A.Kumar; M.Lim; N.Shindo; C.Penn; K. G., Nicholson,N Engl J Med **362**, 1708(2010).

[2] J.Zhou; D.Wang; R.Gao; B.Zhao; JSong.; X.Qi; Y.Zhang; Y.Shi; L.Yang; W.Zhu; T.Bai, K.Qin, Y.Lan, S.Zou, J.Guo, J.Dong, L.Dong, H.Wei, X.Li, J.Lu, L.Liu, X. Zhao, W.Huang, L.Wen, H.Bo;, L.Xin, Y.Chen, C.Xu, Y.Pei, Y.Yang, X.Zhang, S.Wang, Z.Feng, J.Han, W.Yang, G. F.Gao, G.Wu, D.Li, Y.Wang, Y.Shu, Nature **499**, 500(2013).

[3] M. A.Miller, C.Viboud, M.Balinska, L.Simonsen, N Engl J Med **360**, 2595(2009).

[4] Y.Ke, Y.Wang, S.Liu, J.Guo, W.Zhang, X.Yuan, N.Zhang, Z.Wang, H.Song, L.Huang, Z.Chen, Clin Infect Dis **57**, 1506(2013).

[5] M. von Itzstein, Nat. Rev. Drug. Discov. **6**, 967(2007).

[6] S. P.Layne, A. S.Monto, J. K.Taubenberger, Science **323**, 1560(2009).

[7] S.-K.Leang, Y.-M.Deng, R.Shaw, N.Caldwell, P.Iannello, N.Komadina, P.Buchy, M. Chittaganpitch, D. E.Dwyer, P.Fagan, A.-C.Gourinat, F.Hammill, P. F.Horwood, Q. S.Huang, P. K.Ip, L.Jennings, A.Kesson, T.Kok, J. L.Kool, A.Levy, C.Lin, K.Lindsay, O.Osman, G.Papadakis, F.Rahnamal, W.Rawlinson, C.Redden, J.Ridgway, I. C.Sam, S.Svobodova, A.Tandoc, G.Wickramasinghe, J.Williamson, N.Wilson, M. A.Yusof, A.Kelso, I. G.Barr, A. C.Hurt, Antiviral Research **97**, 206(2013).

[8] L. V.Gubareva, L.Kaiser, F. G. Hayden,Lancet **355**, 827(2000).

[9] N. A. Roberts, E. A. Govorkova, The activity of neuraminidase inhibitor oseltamivir against all subtypes of influenza viruses. Nova Science Publishers: New York, 2009; p 93-118.

[10] S.Tong, Y.Li, P.Rivailler, C.Conrardy, D. A.Castillo, L. M.Chen, S.Recuenco, J. A.Ellison, C. T.Davis, I. A.York, A. S.Turmelle, D.Moran, S.Rogers, M.Shi, Y.Tao, M. R.Weil, K.Tang, L. A.Rowe, S.Sammons, X.Xu, M.Frace, K. A.Lindblade, N. J.Cox, L. J.Anderson, C. E.Rupprecht, R. O.Donis, Proc Natl Acad Sci USA **109**, 4269(2012).

[11] J. J.Skehel, D. C.Wiley, Annual Review of Biochemistry **69**, 531(2000).

[12] R.Wagner, M.Matrosovich, H. D.Klenk, Reviews in Medical Virology **12**, 159(2002).

[13] A. K. J.Chong, M. S.Pegg, N. R.Taylor, M. Vonitzstein,Eur. J. Biochem. **207**, 335(1992).

[14] M.Ohuchi, N.Asaoka, T.Sakai, R.Ohuchi, Microbes. Infect. **8**, 1287(2006).

[15] K.Das, J. M.Aramini, L. C.Ma, R. M.Krug, E.Arnold, Nat Struct Mol Biol **17**, 530(2010).

[16] S. S.Chang, H. J.Huang, C. Y.Chen, PLoS Comput Biol **7**, e1002315(2011).

[17] X.Wang, W.Jia, A.Zhao, Phytother Res. **20**, 335(2006).

[18] T.Li, T.Peng, Antivir Res **97**, 1(2013).

[19] Y. B.Ryu, M. J.Curtis-Long, J. H.Kim, S. H.Jeong, M. S.Yang, K. W.Lee, W. S.Lee, K. H.Park, Bioorg. Med. Chem. Lett. **18**, 6046(2008).

[20] R.Li, D.Song, Z.Zhu;, H.Xu, S.Liu, PLoS ONE **7**, e41956(2012).

[21] J.Liu, Z.Yang, S.Wang, L.Liu, G.Chen, L.Wang, J Theor Comput Chem **11**, 111(2012).
[22] Z.Yang, Y.Yang, F.Wu, X.Feng, Mol. Simulat. **39**, 788(2013).
[23] T.-T.Chang, M.-F.Sun, H.-Y.Chen, F.-J.Tsai, M.Fisher, J.-G.Lin, C. Y.-C.Chen, Mol. Simulat. **37**, 361(2011).
[24] T.-T.Chang, M.-F.Sun, H.-Y.Chen, F.-J.Tsai, C. Y.-C.Chen, J Taiwan Inst Chem Eng **42**, 563(2011).
[25] Wu Fei, Y. Z.-W., Yuan Xiao-Hui, Chem J Chinese U **34**, 931(2013).
[26] L. S.Cheng, R. E.Amaro, D.Xu, W. W.Li, P. W.Arzberger, J. A.McCammon, J. Med. Chem. **51**, 3878(2008).
[27] P. M.Colman, Annu Rev Biochem **78**, 95 (2009).
[28] X.Xiong, S. R.Martin, L. F.Haire, S. A.Wharton, R. S.Daniels, M. S.Bennett, J. W.McCauley, P. J.Collins, P. A.Walker, J. J.Skehel, S. J.Gamblin, Nature **499**, 496(2013).
[29] R.Gao, B.Cao, Y.Hu, Z.Feng, D.Wang, W.Hu, J.Chen, Z.Jie, H.Qiu, K.Xu, X.Xu, H.Lu, W.Zhu, Z.Gao, N.Xiang, Y.Shen, Z.He, Y.Gu, Z.Zhang, Y.Yang, X.Zhao, L.Zhou, X.Li, S.Zou, Y.Zhang, X.Li, L.Yang, J.Guo, J.Dong, Q.Li, L.Dong, Y.Zhu, T.Bai, S.Wang, P.Hao, W.Yang, Y.Zhang, J.Han, H.Yu, D.Li, G. F.Gao, G.Wu, Y.Wang, Z.Yuan, Y.Shu, N Engl J Med **368**, 1888(2013).
[30] Accelrys Discovery Studio 3.1. http://accelrys.com.
[31] F.Wu, Z.Yang, X.Yuan, J.Liu, S.Wang, J. Theor. Comput. Chem. **12**, 1350069(2013).
[32] B. J.Smith, P. M.Colman, M.Von Itzstein, B.Danylec, J. N.Varghese, Protein Sci. **10**, 689(2001).
[33] Z. W.Yang, G.Yang, Y. G.Zu, Y. J.Fu, L. J.Zhou, Phys. Chem. Chem. Phys. **11**, 10035(2009).
[34] Z.Yang, Y.Nie, G.Yang, Y.Zu, Y.Fu, L.Zhou, J. Theor. Biol. **267**, 363(2010).
[35] Z. W.Yang, X. M.Wu, Y. G.Zu, G.Yang, L. J.ZHou, Int. J. Quantum. Chem. **112**, 909(2012).
[36] B.Hess, C.Kutzner, D.van der Spoel, E.Lindahl, J. Chem. Theory Comput. **4**, 435(2008).
[37] B. R.Brooks, C. L.Brooks, 3rd; A. D.Mackerell, Jr.; L.Nilsson, R. J.Petrella, B.Roux, Y.Won, G.Archontis, C.Bartels, S.Boresch, A.Caflisch, L.Caves, Q.Cui, A. R.Dinner, M.Feig, S.Fischer, J.Gao, M.Hodoscek, W.Im, K.Kuczera, T.Lazaridis, J.Ma, V.Ovchinnikov, E.Paci, R. W.Pastor, C. B.Post, J. Z.Pu, M.Schaefer, B.Tidor, R. M.Venable, H. L.Woodcock, X.Wu, W.Yang, D. M.York, M.Karplus, J Comput Chem **30**, 1545(2009).
[38] Z.Yang, G.Yang, L.Zhou, J Comput Aided Mol Des **27**, 935(2013).
[39] Y.Li, B.Zhou, R.Wang, J Mol Graph Model **28**, 203(2009).
[40] J. D.Durrant, J. A.McCammon, Comput Biol Chem **34**, 97 (2010).
[41] G.Wu, D. H.Robertson, C. L.Brooks, M.Vieth, J Comput Chem **24**, 1549(2003).
[42] Y. Wang,Bioactivity and active components on green peel of Jugans mandshuricia. Master, Northeast Forestry University, Harbin, 2008.
[43] B. R.Brooks, R. E.Bruccoleri, B. D.Olafson, D. J.States, S.Swaminathan, M.Karplus, J Comput Chem **4**, 187(1983).
[44] H. J. C.Berendsen, D.van der Spoel, R.van Drunen, Comput. Phys. Commun. **91**, 43(1995).
[45] H. J. C.Berendsen, J. P. M.Postma W. F.van Gunsteren, J.Hermans, In: Pullman B, Ed. (Intermolecular forces. Dordrecht: Reidel, 331(1981).

[46] H. J. C.Berendsen, J. P. M.Postma, W. F.van Gunsteren, A.DiNola, J. R.Haak, J Chem Phys **81**, 3684(1984).
[47] T.Darden, D.York, L.Pedersen, J Chem Phys **98**, 10089(1993).
[48] B.Hess, H.Bekker, H. J. C.Berendsen, J. G. E. M.Fraaije, J Comput Chem **18**, 1463(1997).
[49] P.Larsson, B.Wallner, E.Lindahl, A.Elofsson, Protein Sci **17**, 990(2008).
[50] T.Udommaneethanakit, T.Rungrotmongkol, U.Bren, V.Frecer, M.Stanislav, J Chem Inf Model **49**, 2323(2009).
[51] Y. T.Wang, C. H.Chan, Z. Y.Su, C. L.Chen, Biophys Chem **147**, 74(2010).
[52] Y.Mochizuki, K.Yamashita, T.Nakano, Y.Okiyama, K.Fukuzawa, N.Taguchi, S.Tanaka Theor Chem Acc **130**, 515(2011).
[53] A.Grossfield, D. M.Zuckerman, Annual reports in computational chemistry **5**, 23(2009).
[54] Q.Zhang, J.Yang, K.Liang, L.Feng, S.Li, J.Wan, X.Xu, G.Yang, D.Liu, S., Yang, J Chem Inf Model **48**, 1802(2008).
[55] J. N.Varghese, V. C.Epa, P. M.Colman, Protein Sci **4**, 1081(1995).
[56] J. N.Varghese, P. W.Smith, S. L.Sollis, T. J.Blick, A.Sahasrabudhe, J. L.McKimm-Breschkin, P. M.Colman, Structure **6**, 735(1998).
[57] J.Stevens, O.Blixt, T. M.Tumpey, J. K.Taubenberger, J. C.Paulson, I. A.Wilson, Science **312**, 404(2006).
[58] M.Li, B.Wang, Biochem. Biophys. Res. Commun. **347**, 662(2006).
[59] V.Stoll, K. D.Stewart, C. J.Maring, S.Muchmore, V.Giranda, Y.-g. Y.Gu, G.Wang, Y.Chen, M.Sun, C.Zhao, A. L.Kennedy, D. L.Madigan, Y.Xu, A.Saldivar, W.Kati, G.Laver, T.Sowin, H. L.Sham, J.Greer, D.Kempf, Biochemistry **42**, 718(2003).
[60] G.Wu, S.Yan, Biochem. Biophys. Res. Commun. **326**, 475(2005).
[61] O.Aruksakunwong, M.Malaisree, P.Decha, P.Sompornpisut, V.Parasuk, S.Pianwanit, S.Hannongbua, Biophys J **92**, 798(2007).
[62] R. E.Amaro, X.Cheng, I.Ivanov, D.Xu, J. A.McCammon, J. Am. Chem. Soc. **131**, 4702(2009).
[63] J. M.Song, K. H.Lee, B. L.Seong, Antiviral Res. **68**, 66(2005).
[64] J. M.Song, K. D.Park, K. H.Lee, Y. H.Byun, J. H.Park, S. H.Kim, J. H.Kim, B. L.Seong, Antiviral Res. **76**, 178(2007).
[65] T.Eriksson, S.Bjorkman, B.Roth, A.Fyge, P.Hoglund, Chirality **7**, 44(1995).
[66] A.Moscona, N Engl J Med **353**, 1363(2005).
[67] A.Moscona N Engl J Med **360**, 953(2009).
[68] S. J.Gamblin, J. J.Skehel, J Biol Chem **285**, 28403(2010).